Published in final edited form as:
Diabetologia. 2012 November ; 55(11): 2989–2998. doi:10.1007/s00125-012-2678-y.

Degradation of Islet Amyloid Polypeptide by Neprilysin

H. Guan[1,*], **K.M. Chow**[1], **R. Shah**[2], **C.J. Rhodes**[2], and **L.B. Hersh**[1]

[1]Department of Molecular and Cellular Biochemistry, University of Kentucky, Lexington, KY 40536

[2]The Kovler Diabetes Center, Department of Medicine, Section Endocrinology, Diabetes, and Metabolism, University of Chicago, IL 60637

Abstract

Aims/hypothesis—A progressive loss of pancreatic beta-cell function, a decrease in beta-cell mass, and accumulation of islet amyloid is characteristic of type 2 diabetes mellitus. The main constituent of islet amyloid is islet amyloid polypeptide. In this study we have examined the ability of the peptidase neprilysin to cleave human islet amyloid polypeptide and to prevent islet amyloid polypeptide induced pancreatic beta-cell toxicity.

Methods—Neprilysin and a catalytically compromised neprilysin mutant were tested for their ability to inhibit human islet amyloid polypeptide fibrillization and human islet amyloid polypeptide induced pancreatic beta-cell cytotoxicity. Degradation of human islet amyloid polypeptide by neprilysin was followed by high pressure liquid chromatography and the degradation products identified by mass spectrometry.

Results—Neprilysin prevents islet amyloid fibrillization by cleaving islet amyloid polypeptide at Arg^{11}-Leu^{12}, Leu^{12}-Ala^{13}, Asn^{14}-Phe^{15}, Phe^{15}-Leu^{16}, Asn^{22}-Phe^{23} and Ala^{25}-Ile^{26}. In addition neprilysin also appears to prevent human islet amyloid polypeptide fibrillization through a non-catalytic interaction. Neprilysin protected insulinoma cells from exogenously added or endogenously expressed human islet amyloid polypeptide induced beta-cell cytotoxicity.

Conclusions/interpretation—Our data supports a potential therapeutic role for neprilysin in preventing type 2 diabetes mellitus. This study further supports the hypothesis that extracellular human islet amyloid polypeptide contributes to human islet amyloid polypeptide-induced beta-cell cytotoxicity. Whether human islet amyloid polypeptide works through a totally extracellular mechanism or through a cellular reuptake mechanism is unclear at this time.

Keywords

Beta-cell apoptosis; Cleavage; Human islet amyloid polypeptide; Islet amyloid; Neprilysin; Type 2 diabetes mellitus

[*]To whom correspondence should be addressed: Hanjun Guan, Ph.D., Department of Molecular and Cellular Biochemistry, B236 Biomedical Biological Sciences Research Building, 741 South Limestone St., Lexington, KY 40536-0509, USA. Tel: 859-323-6629; Fax: 859-257-2283; hguan2@uky.edu.

Contribution statement: HG and LBH conceived and designed the experiments; HG performed the experiments; HG and LBH analyzed and interpreted the data; HG and LBH wrote the manuscript; KMC, RS and CJR provided reagents. All authors revised the manuscript critically for intellectual content and approved the final version of the paper.

Duality of interest: The authors have declared that there is no duality of interest associated with this manuscript.

Introduction

Type 2 diabetes and Alzheimer's disease (AD) share a number of clinical and biochemical features [1]. Both are characterized by functional tissue loss associated with accumulation and aggregation of a small peptide – islet amyloid polypeptide (IAPP, also known as amylin) in pancreatic islets in type 2 diabetes and amyloid β peptide (Aβ) in AD brain. Human IAPP (hIAPP) aggregation leads to pancreatic beta-cell loss, while Aβ aggregation leads to neuronal cell loss [2, 3]. Similar to the synthesis of Aβ from the amyloid precursor protein (APP), islet amyloid polypeptide is derived from an 89-residue prohormone precursor (preproIAPP) to form the mature 37-amino acid peptide hormone [4]. IAPP is co-secreted with insulin by pancreatic beta-cells [5–7]. hIAPP like human Aβ, but not rodent IAPP (rIAPP) or rodent Aβ, forms oligomers and then fibrils leading to the amyloid deposits seen in association with type 2 diabetes or AD. In the case of IAPP it is thought that three proline residues within the region of amino acids 20–29 of rodent IAPP renders it water soluble and prevents its aggregation. Human IAPP lacks these proline residues and readily aggregates in an aqueous environment [8].

There are several cellular mechanisms to prevent hIAPP accumulation. The unfolded protein response is one such mechanism [2, 9]. Another is to prevent hIAPP accumulation via its degradation by peptidases analogous to the peptidase dependent clearance of Aβ in AD. An up-regulation of synthesis and secretion or a down-regulation of degradation could contribute to hIAPP accumulation and subsequent aggregation. To date insulin-degrading enzyme (IDE) is the only enzyme reported to be able to degrade IAPP [10]. IDE inhibition by bacitracin reportedly impaired IAPP degradation and accelerated amyloid formation in insulinoma cells [10, 11]. More recently, neprilysin (NEP), another amyloid-degrading enzyme, was demonstrated to be involved in the regulation of IAPP aggregation [12, 13] through what was proposed to be a non-catalytic mechanism. NEP has been shown to play a major role in the clearance of Aβ in brain [14] and thus NEP playing a role in preventing IAPP aggregation would represent another parallel between type 2 diabetes and AD.

NEP is present and active in pancreatic islets [13] where its inhibition increased amyloid formation [12]. Conversely, upregulation of NEP decreased amyloid formation and beta-cell apoptosis in cultured hIAPP transgenic mouse islets [12]. However, since NEP degradation of hIAPP was not observed it was suggested that NEP acted by inhibiting hIAPP fibrillization through a non-catalytic protein-protein interaction [12]. In this study we have examined the ability of NEP to cleave hIAPP and to prevent hIAPP induced cell toxicity.

Materials and Methods

Materials

IAPP (1–37, disulfide bridge 2–7, amide) was purchased from Anaspec (Fremont, CA, USA), dissolved in hexafluoride isopropanol (HFIP) and aliquoted. The HFIP was then evaporated using a Speedvac (Thermo Scientific, Waltham, MA, USA) and the powder stored at −80°C. IAPP was freshly dissolved in DMSO (2.5 mmol/l) and diluted in the appropriate buffer or cell culture media prior to use.

Cell culture reagents were from Invitrogen (Carlsbad, CA, USA). Adenoviruses expressing green fluorescent protein (GFP), prepro-rat IAPP-GFP, and prepro-human IAPP-GFP were prepared as previously described [ref]. Glutaryl-Ala-Ala-Phe-4-methoxy-2-naphthylamide (GAAF-4-MNA) and hippuryl-L-phenylalanine and human transferrin were from Sigma (St. Louis, MO, USA). For immunoblotting, the following antibodies were used: rabbit anti-cleaved caspase-3 (Cell Signaling Technology, Danvers, MA, USA) and mouse anti β-actin (EMD Chemicals, Gibbstown, NJ, USA).

Expression and purification of recombinant neprilysin

The ectodomain of human NEP or a catalytically compromised NEP^{E585V} mutant (NEPx) was amplified from plasmid pCSC-SP-PW-NEP or pCSC-SP-PW-NEPx [15] by PCR using the following forward and reverse primers, respectively: 5′-TGAAGGATCCTACGATGATGGTATTTGC-3′ and 5′-TCGAGCGGCCGCTCACCAAACCCGGCACTTCTT-3′. After confirmation by DNA sequencing the PCR products were digested with *Bam*HI/*Not*I and subcloned into the same sites of the expression vector psGHP1. The psGHP1 vector contains a human growth hormone (GH) domain and an octahistidine affinity tag [16] followed by a PreScission protease cleavage site into vector pLEXm [17]. CHO-S cells transfected with psGHP1-NEP or psGHP1-NEPx were cultured for 4 days and the supernatant collected and concentrated with a Pellicon tangential flow filtration system (Millipore, Billerica, MA, USA). His-Tagged NEP or NEPx-human growth hormone fusion proteins were purified using HIS-Select Nickel Affinity Gel (Sigma, St. Louis, MO, USA).

Growth hormone was removed by PreScission protease digestion overnight at 4°C. The proteins were then applied to a MonoQ CEX anion exchange column in 20 mmol/l Tris·HCl buffer (pH 7.4) and eluted with a 0–0.5 mol/l linear NaCl gradient. NEP was eluted at ~0.15 mol/l NaCl. The NEP containing fractions were pooled and concentrated with a Millipore Centricon concentrator and store at −80°C in 20% glycerol. The purity of recombinant proteins was determined using NIH Image J software [18] to analyze Coomassie blue stained gels subjected to sodium dodecyl sulfate-polyacrylamide gel electrophoresis (SDS-PAGE).

Fluorogenic assay of NEP activity

NEP activity was determined with the fluorogenic substrate glutaryl-Ala-Ala-Phe-4-methoxy-2-naphthylamide (GAAF-4-MNA) (Sigma, St. Louis, MO, USA) [15]. Reaction mixtures (200 μl) contained 100 μmol/l GAAF-4-MNA, 1μg recombinant puromycin-sensitive aminopeptidase (PSA) and 20 mmol/l 2-(N-morpholino)ethanesulfonic acid (MES) buffer, pH 6.5. Reactions were initiated by the addition of enzyme and monitored continuously at 37°C at an excitation wavelength of 340 nm and an emission wavelength of 425 nm using a SpectraMAX GeminiXS Microplate reader (Molecular devices, Sunnyvale, CA, USA). In this assay GAAF-4-MNA is cleaved by NEP to release F-4-MNA, which is then converted to the fluorescent 4-MNA by excess PSA [19].

Carboxypeptidase activity assay

Carboxypeptidase activity was determined using 100μmol/l Hippuryl-L-phenylalanine as substrate with the generation of hippuric acid monitored at 254 nm at 25°C [20]. The same concentration of NEP and the same buffer used in measuring NEP dependent hIAPP degradation were used in this assay.

Thioflavin T assay

The fibrillization of hIAPP was monitored using Thioflavin T as described previously with minor modifications [12]. hIAPP was dissolved in DMSO (2.5 mmol/l) and then diluted into 25 mmol/l Tris·HCl buffer, pH 8.0, containing 100 mmol/l NaCl to give a final concentration of 50 μmol/l hIAPP and 2% DMSO. A 1 μmol/l stock of recombinant human NEP or NEPx was prepared in the same buffer. Reactions were initiated by mixing equal amounts of the hIAPP stock with the NEP stock. In control experiments, 1 μmol/l NEP was preincubated with 50 μmol/l of the NEP inhibitor phosphoramidon for 30 min. Preliminary experiments confirmed greater than 99% inhibition of NEP activity under this condition. Reactions were placed in a 37°C incubator in the dark with gentle rocking for 20 h.

Thioflavin T was added to the mixture to a final concentration of 5 μmol/l and its fluorescence measured at 437 nm excitation and 482 nm emission wavelengths after mixing. Bovine serum albumin (BSA) and transferrin were used as protein controls.

Transmission electron microscopy (TEM)

The fibrillization of hIAPP was examined by transmission electron microscopy using samples at the end of the thioflavin T experiments (at $t = 20$ h) as previously described [12, 21].

Cell culture

The rat insulinoma cell line INS 832/13, kindly provided by Dr. Christopher Newgard (Duke University, Durham, NC, USA) [22], was cultured at 37°C and 5% CO_2 in RPMI 1640 medium supplemented with 11.1 mmol/l glucose, 10% FBS, 10 mmol/l HEPES, 2 mmol/l L-glutamine, 1 mmol/l sodium pyruvate, 50 μmol/l 2-mercaptoethanol and 100 units/ml penicillin plus 100 μg/ml streptomycin. For cytotoxicity studies, cells were treated with 20 μmol/l hIAPP and purified NEP or NEPx. Cytotoxicity was analyzed using the methylthiazolyldiphenyl-tetrazolium bromide (MTT) assay [23] as well as by measuring the cleavage and activation of caspase-3 [24, 25], which is the key downstream enzyme in apoptosis induced by hIAPP in pancreatic beta-cells [2, 25]. In another paradigm cells were transduced with adenovirus expressing prepro-hIAPP-GFP at a multiplicity of infection (MOI) of 100 and cultured for 48 hours. Adenovirus expressing GFP or prepro-rIAPP-GFP at the same MOI were used as controls. Cell cytotoxicity was analyzed as above.

MTT assay

For determining cell viability an MTT stock solution (5 mg/ml in PBS) was added at 1:10 (vol/vol) to the culture medium. After incubation in the dark at 37°C for 4 h, the supernatant was removed and 0.4N HCl in isopropanol (1 culture volume) was added. The plates were kept in the dark at room temperature for 1 h and then the absorbance at 570 nm measured. Cell viability was calculated as the percentage of the absorbance of experimentally treated cells compared to the absorbance of a vehicle control [23].

Western blot analysis

Protein concentration was determined using the BCA protein assay kit (Thermo Scientific, Rockford, IL, USA) with bovine serum albumin as a standard. Cell lysates containing 25 μg of total protein were separated on a 4–12% Bis-Tris NuPAGE gel (Invitrogen, Carlsbad, CA, USA) and transferred to polyvinylidine fluoride (PVDF) membranes (Bio-Rad, Hercules, CA, USA). Membranes were blocked with 5% nonfat dry milk in Tris-buffered saline (TBS)/0.1% Tween-20 and incubated overnight at 4°C with one of the following primary antibodies: goat anti-cleaved caspase-3 (1:1,000) and mouse anti-β-actin (1:10,000). Membranes were washed with TBS/0.1% Tween-20, incubated with the corresponding horseradish peroxidase (HRP)-conjugated secondary antibody (Zymed Laboratories, San Francisco, CA, USA), followed by ECL-Plus (GE Healthcare, Piscataway, NJ, USA) detection. Protein expression levels were quantified using NIH ImageJ software [18]. Membranes were reprobed after stripping.

Cleavage of hIAPP by neprilysin

20 μmol/l hIAPP was incubated with NEP or NEPx in 20 mmol/l MES buffer, pH 6.5, at 37°C. Reactions were stopped by addition of trifluoroacetic acid (TFA) to 0.5% and then analyzed by reverse phase HPLC on a Vydac C4 column. Fractions were separated by a linear gradient from 0.1% TFA in 90% water/10% acetonitrile to 0.1% TFA in 50% water/50% acetonitrile [26]. hIAPP or its cleavage products were collected manually and identified

by mass spectrometry using an Applied Biosystems 4800 MALDI TOF/TOF Proteomics Analyzer. Additionally reaction mixtures, after being stopped with TFA and bound to and eluted from a C18 mini column, were analyzed directly in the mass spectrometer. These analyses were performed at the University of Kentucky Proteomics Core Facility.

Statistical analysis

Data were expressed as the mean ± SEM and compared using one-way ANOVA followed by Dunnett's multiple comparison test for statistical significance. Values with a $p< 0.05$ are considered statistically significant.

Results

The effect of NEP and catalytically compromised NEPx on hIAPP fibrillization

Recombinant human NEP and its catalytically compromised NEP^{E585V} mutant (NEPx) were expressed as their secreted catalytic ectodomain using CHO-S cells and purified by Ni-affinity chromatography and anion exchange chromatography. The calculated molecular weight of the NEP ectodomain is 83kDa, while the apparent molecular weight on SDS-PAGE is ~95kDa due to glycosylation. NEP purity was greater than 95% as judged by Coomassie blue staining of an SDS-PAGE gel (Fig. 1A) while that of NEPx was ~80%. The major contamination in the NEPx preparation is bovine transferrin (TF), molecular weight of 75 kDa, which was identified by MALDI TOF/TOF. As noted below, transferrin did not affect hIAPP aggregation or hIAPP-induced cytotoxicity. The activity of NEP and NEPx were determined using the fluorogenic substrate GAAF-4-MNA, Fig. 1B. The E585V mutation abolished greater than 98% of the NEP activity as previously reported [27]. The NEP inhibitor phosphoramidon (PA) reduced the activity of NEP and NEPx to undetectable levels (Fig. 1B).

We initially sought to confirm and extend the report that NEP impedes islet amyloid formation by inhibition of fibril formation through protein-protein interactions [12]. Thus the ability of the catalytically compromised NEPx and active NEP to inhibit hIAPP fibril formation was compared. NEPx retains the same substrate binding affinity as wild-type NEP [27] while as noted above loses >98% of its enzymatic activity. This form of NEP, like NEP itself, should be capable of preventing hIAPP fibrillization through protein-protein interactions. We measured hIAPP fibrillization in the presence of either 0.5 μmol/l NEP or 0.5 μmol/l NEPx as described by Zraika *et al.* [12]. Fibrillization was monitored at various time-points to get a complete picture of the kinetics of the process. NEP or NEPx treated with 50 μmol/l phosphoramidon (PA) or the same molar concentration of BSA or transferrin (TF) served as controls. As shown in Fig. 2A, hIAPP undergoes fibrillization after 6 h and reaches a maximum after 9 h as indicated by the increase in thioflavin T fluorescence. TF, BSA, PA treated-NEP, and NEPx all delayed hIAPP fibrillization as thioflavin T fluorescence did not increase until 9 h, but reached the same maxima as the untreated control after 12 h. We interpret this effect to represent a nonspecific inhibitory effect of protein on hIAPP fibrillogenesis. In contrast, NEP completely inhibited hIAPP fibril formation over the entire 20 h incubation period. However, the addition of the same amount of NEPx slightly delayed hIAPP fibrillization more than BSA or TF indicating the contribution of its residual activity.

To exclude the possibility that the added proteins or phosphoramidon interfered with the thioflavin T assay [21], electron microscopy was used to confirm fibril formation at the 20 h time point. As shown in Fig. 2B, hIAPP fibrils were observed in the untreated hIAPP (CTRL), NEPx, and TF samples. Fibrils were also seen in BSA, PA-treated NEP and PA-

treated NEPx samples (data not shown). In contrast fibrils were not seen with NEP treated hIAPP.

NEP cleaves hIAPP *in vitro*

The ability of NEP to prevent hIAPP fibrillization and the absence of an effect of catalytically compromised NEPx suggests that NEP impedes islet amyloid formation by degrading hIAPP. We thus tested the ability of NEP to cleave hIAPP by incubating 20μmol/l hIAPP with 400 nmol/l NEP or NEPx at 37°C for 1 h. Reactions were terminated by the addition of TFA to a final concentration of 0.5% and then analyzed by reverse-phase HPLC. As shown in Fig. 3A, the hIAPP peak decreased more than 70% after the 1 h incubation period and a number product peaks were observed. hIAPP cleavage was blocked by the NEP inhibitor phosphoramidon (Fig. 3B). In addition no cleavage of hIAPP was observed with NEPx under identical reaction conditions (Fig. 3C), clearly demonstrating that NEP cleaves hIAPP.

To identify the NEP cleavage sites, hIAPP was incubated with NEP at 37°C for 60 min and products separated by HPLC. Peaks were manually collected and subjected to mass spectral analysis for identification. Cleavage of hIAPP by NEP was detected at Arg^{11}-Leu^{12}, Leu^{12}-Ala^{13}, Asn^{14}-Phe^{15}, Phe^{15}-Leu^{16} and Ala^{25}-Ile^{26}, Fig. 4. The C-terminal product of the Ala^{25}-Ile^{26} cleavage (ILSSTNVGSNTY-NH_2) appeared to be further cleaved as this product initially increased with time, but then decreased at latter times (Fig. 5A). The two major products were the amino-terminal peptides $hIAPP^{1–11}$ and $hIAPP^{1–12}$ (peak 4 and 7 in the HPLC chromatogram, Fig. 4). We were unable to identify peaks #1–3, Fig. 4. We confirmed cleavage sites by direct measure of the reaction products by mass spectrometry without prior separation by HPLC. Additional products KCNTATCATQRLANF, KCNTATCATQRLANFLVHSSNNFGA, KCNTATCATQRLANFLVHSSNN, and LANFLVHSSNNFGAILSSTNBGSNTY-NH2 were found by direct analysis. All of these cleavage sites are consistent with the known specificity of NEP which cleaves on the amino side of non-polar residues [28].

Cleavage sites in rat IAPP were identified at Arg^{11}-Leu^{12}, Leu^{12}-Ala^{13}, Asn^{14}- Phe^{15} and Phe^{15}-Leu^{16}, which are identical to human IAPP cleavage sites. No cleavage was observed at Asn^{22}-Leu^{23} and Pro^{26}-Val^{27} in rat IAPP which corresponds to Asn^{22}-Phe^{23} and Ala^{26}-Ile^{27} in human IAPP, likely attributed to the amino acid differences between rat and human IAPP. Since four of the cleavage products were clustered together we considered the possibility that these may be derived by secondary cleavage by a contaminating carboxypeptidase acting on KCNTATCATQRLANF. We thus assayed for carboxypeptidases activity in the NEP preparations, but no such activity was detected.

Comparison of NEP cleavage of hIAPP to $Aβ_{1–40}$

Since $Aβ_{1–40}$ is a well-known substrate for NEP [14, 29, 30], we compared its degradation to that of hIAPP. Rates of peptide hydrolysis were determined by measuring disappearance of the hIAPP or $Aβ_{1–40}$ peak by HPLC, (Fig. 5A and Fig. 5B). The The logarithm of the percentage of substrate remaining was plotted as a function of time for the linear range (Fig. 5C) showed that the rate of $Aβ_{1–40}$ cleavage is 0.305 ± 0.041 nmols/min/μg NEP while that for hIAPP is 0.010 ± 0.002 nmols/min/μg NEP. Thus NEP cleaves $Aβ_{1–40}$ approximately 30 times faster than it cleaves hIAPP.

The effect of exogenous NEP and NEPx on hIAPP-induced cytotoxicity of pancreatic beta-cells

The effects of recombinant NEP or NEPx on hIAPP-induced cytotoxicity were examined using the INS 832/13 insulinoma cell line. Cells were treated with 20μM synthetic hIAPP in

the presence of NEP or NEPx, and cell viability determined 48 h after treatment using the MTT assay. As shown in Fig. 6A, there were 15.6 ± 3.5% viable cells in cells treated for 48 h with 20 μmol/l hIAPP relative to vehicle control cells (CTRL). As expected rat IAPP did not cause significant cytotoxicity. The addition of 400 nmol/l or 40 nmol/l NEP blocked hIAPP-induced cytotoxicity (84.5 ± 7.3% viable cells in the presence of 400 nmol/l NEP and 92.9 ± 9.5% viable cells in the presence 40nmol/l NEP), while 4 nmol/l NEP increased the cell viability to 39.4 ± 15.3% although a statistically significant value was not reached. By contrast, only 400 nmol/l NEPx significantly increased cell viability (58.4 ± 9.3%). The addition of 400 nmol/l TF in the culture media did not protect beta-cells against synthetic hIAPP-induced cytotoxicity. Additionally, the effect of NEP on synthetic hIAPP-induced apoptosis was evaluated by measuring the cleavage and activation of caspase-3 [24, 25]; the key downstream enzyme in hIAPP induced apoptosis in pancreatic beta-cells [2, 25]. hIAPP, but not rIAPP, induced apoptosis in INS832/13 cells as indicated by the increase in cleaved caspase-3 (Fig. 6B). The ratio of cleaved caspase-3/actin induced by synthetic hIAPP decreased by 67% and 95% with 40 nmol/l or 400 nmol/l NEP, respectively. However, neither 4 nmol/l NEP, 400 nmol/l NEPx, nor 400 nmol/l TF protected against hIAPP-induced apoptosis. To further study the effect of NEP on hIAPP-induced cytotoxicity, the precursor to hIAPP, prepro-hIAPP, was expressed in INS 832/13 cells. Cells were transduced with adenovirus expressing prepro-hIAPP fused with a GFP tag at an MOI of 100 [24]. As previously reported [24] prepro-IAPP-GFP is processed by prohormone convertases PC1/3 and PC2 to form mature IAPP in INS 832/13 cells. As controls, the cells were also treated with same MOI of adenovirus expressing prepro-rIAPP-GFP and GFP. The MTT assay and cleaved caspase-3 levels were measured to determine the effects of recombinant NEP and NEPx on the hIAPP overexpression-induced beta-cell cytotoxicity. As shown in Fig. 7A, overexpression of hIAPP, but not rIAPP or GFP, induced cytotoxicity in INS 832/13 cells. The addition of 400 nmol/l NEP reduced this hIAPP induced cytotoxicity, however lower concentrations of NEP, NEPx, or TF had no effect on the hIAPP induced cytotoxicity. Furthermore, overexpression of hIAPP, but not rIAPP or GFP, by adenovirus transduction induced apoptosis as indicated by an increase in cleaved caspase-3, Fig. 7B. Addition of NEP to the media dramatically decreased the amount of activated caspase-3. The normalized ratio of cleaved caspase-3/actin was decreased by 28%, 59% and 78% with 4, 40 nmol/l or 400 nmol/l recombinant NEP, respectively. For NEPx, only 400 nmol/l NEPx treatment reduced hIAPP induced apoptosis. No effect on hIAPP-induced apoptosis was observed with cells treated with 4 or 40 nmol/l NEPx or 400 nmol/l TF (Fig. 7C).

Discussion

In the current study, the ability of wild-type NEP and a catalytically compromised NEP^{E585V} mutant (NEPx) to inhibit hIAPP fibrillization and hIAPP induced cytotoxicity were compared. NEPx retains the same substrate binding affinity as wild-type NEP [27], while as noted above loses >98% of its enzymatic activity. NEP could completely prevent hIAPP fibril formation as measured by both thioflavin T assay and electron microscopy. NEPx could delay fibrillization, but could not completely inhibit hIAPP fibrillization in what appears to be primarily a non-specific effect of protein. In cytotoxicity studies, the concentration of NEPx required preventing synthetic hIAPP or hIAPP overexpression-induced cytotoxicity was much higher than that of NEP in an insulinoma cells.

We have shown that NEP degrades hIAPP, although slowly compared to Aβ. This differs from the study of Zraika *et al.* [12] in which it was concluded that NEP did not cleave hIAPP. Since NEP cleaves Aβ thirty times faster than hIAPP (Fig. 5C), it is quite possible that in the study of Zraika *et al.* they used a sufficient amount of enzyme to observe Aβ cleavage, but not enough enzyme to see IAPP cleavage.

Taken together, these data suggests that there are two mechanisms whereby NEP can block hIAPP fibril formation. The first is a non-catalytic mechanism as proposed by Zraika *et al.* [12] in which NEP interacts with hIAPP through a not-yet-defined protein-protein interaction(s). This appears to be a non-specific effect as transferrin and BSA are as effective as phosphoramidon treated-NEP in inhibiting fibril formation. In addition relative high protein concentrations were required to see this effect. The second mechanism is through the catalytic cleavage of hIAPP. This latter mechanism is in keeping with the ability of NEP to degrade Aβ [14, 29, 30], another fibril forming peptide.

Previous studies have suggested that neprilysin is present and active in islets, including beta-cells and may play a role in regulating islet amyloid accumulation [13]. Thus much like the role of NEP in preventing amyloid accumulation in AD, NEP could prevent hIAPP aggregation in pancreatic beta-cells. Hence NEP based therapeutic strategies for preventing type 2 diabetes are worthy of consideration.

Whether the toxic species of hIAPP are formed intracellularly or extracellularly or both remain ambiguous. Initially it was thought that hIAPP co-secreted with insulin could aggregate extracellularly to form oligomers and then fibrils leading to mature amyloid deposits [31]. It was thought that these insoluble mature hIAPP amyloid deposits cause pancreatic beta-cell loss since amyloid deposits were found in the majority of individuals with type 2 diabetes [32–34]. Furthermore the extent of extracellular amyloid deposition correlated with beta-cell apoptosis and beta-cell loss [35] as well as clinical severity of the diabetes [36]. However, several recent studies suggested that it is soluble hIAPP oligomers rather than insoluble amyloid deposits that represent the main cytotoxic species [2, 37–41]. It was also recently proposed that hIAPP aggregation starts intracellularly [2, 42]. hIAPP oligomers were detected intracellularly in beta-cells of hIAPP transgenic mice [38, 39] as well as in individuals with type 2 diabetes [39]. Since vaccine induced high titers of anti hIAPP oligomer antibodies in transgenic mice failed to prevent, but instead exacerbated beta-cell apoptosis and diabetes onset, it was suggested that hIAPP induced toxicity in hIAPP transgenic mice is likely initiated intracellularly and that the IAPP may not be accessible to anti-oligomer antibodies [38]. However, how intracellular hIAPP accumulates and aggregates remains a key question to be addressed. A recent study suggested that exogenous hIAPP could be internalized by beta-cells which is regulated by plasma membrane cholesterol levels [43]. The finding in the present study that NEP added to the cell media prevents hIAPP induced apoptosis from endogenously expressed hIAPP shows that at least in a cell model extracellular hIAPP contributes to hIAPP-induced death. Since exogenous NEP would not be able to enter cells, this shows that extracellular hIAPP secreted by INS 832/13 cells plays a role in hIAPP induced apoptosis. This is consistent with the previous report showing hIAPP release is necessary for islet amyloid formation and its toxic effects [44]. It is interesting that islet beta-cells are reportedly more susceptible to extracellular hIAPP toxicity than alpha-cells cultured [25], however additional studies are required to verify the underlying mechanisms. Unfortunately, our results do not distinguish between hIAPP aggregating extracellularly and inducing cell death and hIAPP being secreted and re-entering the cells. In both cases extracellular NEP reduces the concentration of extracellular IAPP and thus would affect either process.

Taken together, this study demonstrates the hIAPP degrading activity of NEP and its protective effects against hIAPP induced pancreatic beta-cells apoptosis. This study also highlights the potential of degrading extracellular hIAPP by NEP or other hIAPP degrading enzymes as a therapeutic approach for type 2 diabetes.

Acknowledgments

The authors thank Dr. Craig Vander Kooi for technical assistance for the expression and purification of neprilysin using CHO-S cells. We are grateful to Dr. Christopher Newgard for supplying insulinoma cell line INS 832/13. Mass spectrometric analyses were performed by Dr. Carol Beach at the University of Kentucky Center for Structural Biology Proteomics Core Facility, which is supported in part by grant P20RR020171 from the NIH/NCRR. This work was supported in part by grants from the National Institutes of Health RO1DA02243 and P20RR020171 (L.B.H).

Abbreviations

4-MNA	4-methoxy-2-naphthylamide
Aβ	Amyloid β peptide
AD	Alzheimer's disease
HFIP	Hexafluoride isopropanol
hIAPP	Human islet amyloid polypeptide
IAPP	Islet amyloid polypeptide
MES	2-(N-morpholino)ethanesulfonic acid
MTT	Methylthiazolyldiphenyl-tetrazolium bromide
NEP	Neprilysin
NEPx	Catalytically compromised NEP ^{E585V} mutant
rIAPP	Rodent islet amyloid polypeptide
TF	Trasferrin
TFA	Trifluoroacetic acid
PA	Phosphoramidon

References

1. Gotz J, Ittner LM, Lim YA. Common features between diabetes mellitus and Alzheimer's disease. Cell Mol Life Sci. 2009; 66:1321–1325. [PubMed: 19266159]
2. Haataja L, Gurlo T, Huang CJ, Butler PC. Islet amyloid in type 2 diabetes, and the toxic oligomer hypothesis. Endocr Rev. 2008; 29:303–316. [PubMed: 18314421]
3. Hardy J, Selkoe DJ. The amyloid hypothesis of Alzheimer's disease: progress and problems on the road to therapeutics. Science. 2002; 297:353–356. [PubMed: 12130773]
4. Sanke T, Bell GI, Sample C, Rubenstein AH, Steiner DF. An islet amyloid peptide is derived from an 89-amino acid precursor by proteolytic processing. J Biol Chem. 1988; 263:17243–17246. [PubMed: 3053705]
5. Kahn SE, D'Alessio DA, Schwartz MW, et al. Evidence of cosecretion of islet amyloid polypeptide and insulin by beta-cells. Diabetes. 1990; 39:634–638. [PubMed: 2185112]
6. Moore CX, Cooper GJ. Co-secretion of amylin and insulin from cultured islet beta-cells: modulation by nutrient secretagogues, islet hormones and hypoglycemic agents. Biochem Biophys Res Commun. 1991; 179:1–9. [PubMed: 1679326]
7. Butler PC, Chou J, Carter WB, et al. Effects of meal ingestion on plasma amylin concentration in NIDDM and nondiabetic humans. Diabetes. 1990; 39:752–756. [PubMed: 2189768]
8. Westermark P, Engstrom U, Johnson KH, Westermark GT, Betsholtz C. Islet amyloid polypeptide: pinpointing amino acid residues linked to amyloid fibril formation. Proc Natl Acad Sci U S A. 1990; 87:5036–5040. [PubMed: 2195544]
9. Scheuner D, Kaufman RJ. The unfolded protein response: a pathway that links insulin demand with beta-cell failure and diabetes. Endocr Rev. 2008; 29:317–333. [PubMed: 18436705]

10. Bennett RG, Duckworth WC, Hamel FG. Degradation of amylin by insulin-degrading enzyme. J Biol Chem. 2000; 275:36621–36625. [PubMed: 10973971]
11. Bennett RG, Hamel FG, Duckworth WC. An insulin-degrading enzyme inhibitor decreases amylin degradation, increases amylin-induced cytotoxicity, and increases amyloid formation in insulinoma cell cultures. Diabetes. 2003; 52:2315–2320. [PubMed: 12941771]
12. Zraika S, Aston-Mourney K, Marek P, et al. Neprilysin impedes islet amyloid formation by inhibition of fibril formation rather than peptide degradation. J Biol Chem. 2010; 285:18177–18183. [PubMed: 20400513]
13. Zraika S, Hull RL, Udayasankar J, et al. Identification of the amyloid-degrading enzyme neprilysin in mouse islets and potential role in islet amyloidogenesis. Diabetes. 2007; 56:304–310. [PubMed: 17259373]
14. Hersh LB, Rodgers DW. Neprilysin and amyloid beta peptide degradation. Curr Alzheimer Res. 2008; 5:225–231. [PubMed: 18393807]
15. Guan H, Liu Y, Daily A, et al. Peripherally expressed neprilysin reduces brain amyloid burden: a novel approach for treating Alzheimer's disease. J Neurosci Res. 2009; 87:1462–1473. [PubMed: 19021293]
16. Leahy DJ, Dann CE 3rd, Longo P, Perman B, Ramyar KX. A mammalian expression vector for expression and purification of secreted proteins for structural studies. Protein Expr Purif. 2000; 20:500–506. [PubMed: 11087690]
17. Aricescu AR, Lu W, Jones EY. A time-andcost-efficient system for high-level protein production in mammalian cells. Acta Crystallogr D Biol Crystallogr. 2006; 62:1243–1250. [PubMed: 17001101]
18. Abramoff MD, Magelhaes PJ, Ram SJ. Image processing with imagej. Biophotonics Int. 2004; 11:36–42.
19. Daily A, Nath A, Hersh LB. Tat peptides inhibit neprilysin. J Neurovirol. 2006; 12:153–160. [PubMed: 16877296]
20. Folk JE, Schirmer EW. The Porcine Pancreatic Carboxypeptidase a System. I. Three Forms of the Active Enzyme. J Biol Chem. 1963; 238:3884–3894. [PubMed: 14086721]
21. Meng F, Marek P, Potter KJ, Verchere CB, Raleigh DP. Rifampicin does not prevent amyloid fibril formation by human islet amyloid polypeptide but does inhibit fibril thioflavin-T interactions: implications for mechanistic studies of beta-cell death. Biochemistry. 2008; 47:6016–6024. [PubMed: 18457428]
22. Hohmeier HE, Mulder H, Chen G, Henkel-Rieger R, Prentki M, Newgard CB. Isolation of INS-1-derived cell lines with robust ATP-sensitive K+ channel-dependent and -independent glucose-stimulated insulin secretion. Diabetes. 2000; 49:424–430. [PubMed: 10868964]
23. Liu Y, Peterson DA, Kimura H, Schubert D. Mechanism of cellular 3-(4,5-dimethylthiazol-2-yl)-2,5-diphenyltetrazolium bromide (MTT) reduction. J Neurochem. 1997; 69:581–593. [PubMed: 9231715]
24. Huang CJ, Lin CY, Haataja L, et al. High expression rates of human islet amyloid polypeptide induce endoplasmic reticulum stress mediated beta-cell apoptosis, a characteristic of humans with type 2 but not type 1 diabetes. Diabetes. 2007; 56:2016–2027. [PubMed: 17475933]
25. Law E, Lu S, Kieffer TJ, et al. Differences between amyloid toxicity in alpha and betacells in human and mouse islets and the role of caspase-3. Diabetologia. 2010; 53:1415–1427. [PubMed: 20369225]
26. Chow KM, Gakh O, Payne IC, et al. Mammalian pitrilysin: substrate specificity and mitochondrial targeting. Biochemistry. 2009; 48:2868–2877. [PubMed: 19196155]
27. Devault A, Nault C, Zollinger M, et al. Expression of neutral endopeptidase (enkephalinase) in heterologous COS-1 cells. Characterization of the recombinant enzyme and evidence for a glutamic acid residue at the active site. J Biol Chem. 1988; 263:4033–4040. [PubMed: 2894375]
28. Li C, Hersh LB. Neprilysin: assay methods, purification, and characterization. Methods Enzymol. 1995; 248:253–263. [PubMed: 7674925]
29. Howell S, Nalbantoglu J, Crine P. Neutral endopeptidase can hydrolyze beta-amyloid(1–40) but shows no effect on beta-amyloid precursor protein metabolism. Peptides. 1995; 16:647–652. [PubMed: 7479298]

30. Iwata N, Tsubuki S, Takaki Y, et al. Metabolic regulation of brain Abeta by neprilysin. Science. 2001; 292:1550–1552. [PubMed: 11375493]

31. Johnson KH, O'Brien TD, Betsholtz C, Westermark P. Islet amyloid, islet-amyloid polypeptide, and diabetes mellitus. N Engl J Med. 1989; 321:513–518. [PubMed: 2668761]

32. Butler AE, Janson J, Bonner-Weir S, Ritzel R, Rizza RA, Butler PC. Beta-cell deficit and increased beta-cell apoptosis in humans with type 2 diabetes. Diabetes. 2003; 52:102–110. [PubMed: 12502499]

33. Zhao HL, Lai FM, Tong PC, et al. Prevalence and clinicopathological characteristics of islet amyloid in chinese patients with type 2 diabetes. Diabetes. 2003; 52:2759–2766. [PubMed: 14578294]

34. Clark A, Wells CA, Buley ID, et al. Islet amyloid, increased A-cells, reduced B-cells and exocrine fibrosis: quantitative changes in the pancreas in type 2 diabetes. Diabetes Res. 1988; 9:151–159. [PubMed: 3073901]

35. Jurgens CA, Toukatly MN, Fligner CL, et al. beta-cell loss and beta-cell apoptosis in human type 2 diabetes are related to islet amyloid deposition. Am J Pathol. 2011; 178:2632–2640. [PubMed: 21641386]

36. Schneider HM, Storkel S, Will W. Amyloid of islets of Langerhans and its relation to diabetes mellitus (author's transl). Dtsch Med Wochenschr. 1980; 105:1143–1147. [PubMed: 7004825]

37. Janson J, Ashley RH, Harrison D, McIntyre S, Butler PC. The mechanism of islet amyloid polypeptide toxicity is membrane disruption by intermediate-sized toxic amyloid particles. Diabetes. 1999; 48:491–498. [PubMed: 10078548]

38. Lin CY, Gurlo T, Kayed R, et al. Toxic human islet amyloid polypeptide (h-IAPP) oligomers are intracellular, and vaccination to induce anti-toxic oligomer antibodies does not prevent h-IAPP-induced beta-cell apoptosis in h-IAPP transgenic mice. Diabetes. 2007; 56:1324–1332. [PubMed: 17353506]

39. Gurlo T, Ryazantsev S, Huang CJ, et al. Evidence for proteotoxicity in beta cells in type 2 diabetes: toxic islet amyloid polypeptide oligomers form intracellularly in the secretory pathway. Am J Pathol. 2010; 176:861–869. [PubMed: 20042670]

40. Konarkowska B, Aitken JF, Kistler J, Zhang S, Cooper GJ. The aggregation potential of human amylin determines its cytotoxicity towards islet beta-cells. Febs J. 2006; 273:3614–3624. [PubMed: 16884500]

41. Meier JJ, Kayed R, Lin CY, et al. Inhibition of human IAPP fibril formation does not prevent beta-cell death: evidence for distinct actions of oligomers and fibrils of human IAPP. Am J Physiol Endocrinol Metab. 2006; 291:E1317–1324. [PubMed: 16849627]

42. Westermark P, Andersson A, Westermark GT. Islet amyloid polypeptide, islet amyloid, and diabetes mellitus. Physiol Rev. 2011; 91:795–826. [PubMed: 21742788]

43. Trikha S, Jeremic AM. Clusteringand internalization of toxic amylin oligomers in pancreatic cells requires plasma membrane cholesterol. J Biol Chem. 2011

44. Aston-Mourney K, Hull RL, Zraika S, Udayasankar J, Subramanian SL, Kahn SE. Exendin-4 increases islet amyloid deposition but offsets the resultant beta cell toxicity in human islet amyloid polypeptide transgenic mouse islets. Diabetologia. 2011; 54:1756–1765. [PubMed: 21484213]

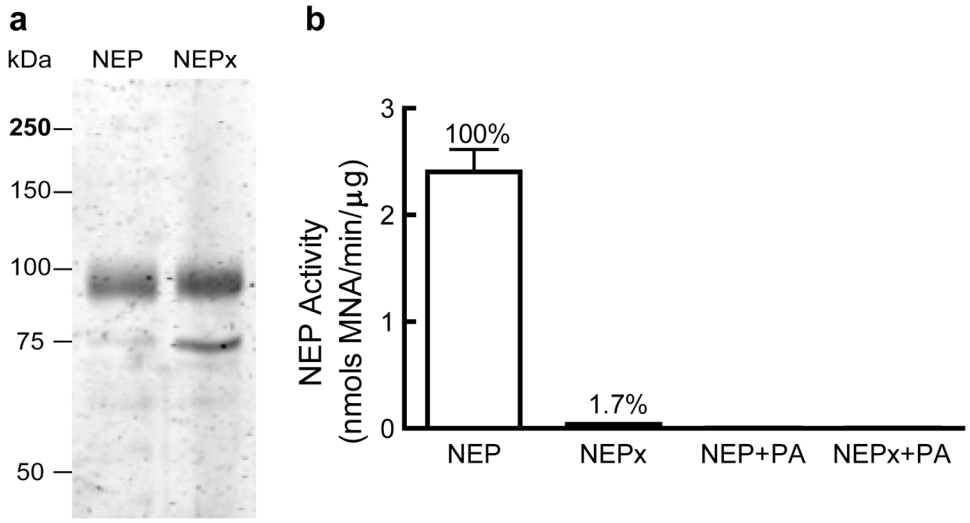

Fig. 1. Purified recombinant neprilysin (NEP) and a catalytically compromised NEP^{E585V} mutant (NEPx)

a. Recombinant NEP and NEPx were purified by nickel affinity and anion exchange chromatography as described in Materials and Methods and analyzed by SDS-PAGE on a 10% polyacrylamide gel stained with Coomassie blue. The purity of recombinant NEP is greater than 95% while the purity of recombinant NEPx is about 80%. The 75kDa protein contaminant in the NEPx preparation was identified as bovine transferrin by MALDI TOF/TOF.

b. Activity of recombinant NEP, NEPx, NEP in the presence of phosphoramidon, and NEPx in the presence of phosphoramidon as determined with GAAF-4-MNA as substrate. NEPx exhibits ~1.7% of wild-type NEP activity. Phosphoramidon decreased NEP and NEPx activity to undetectable levels.

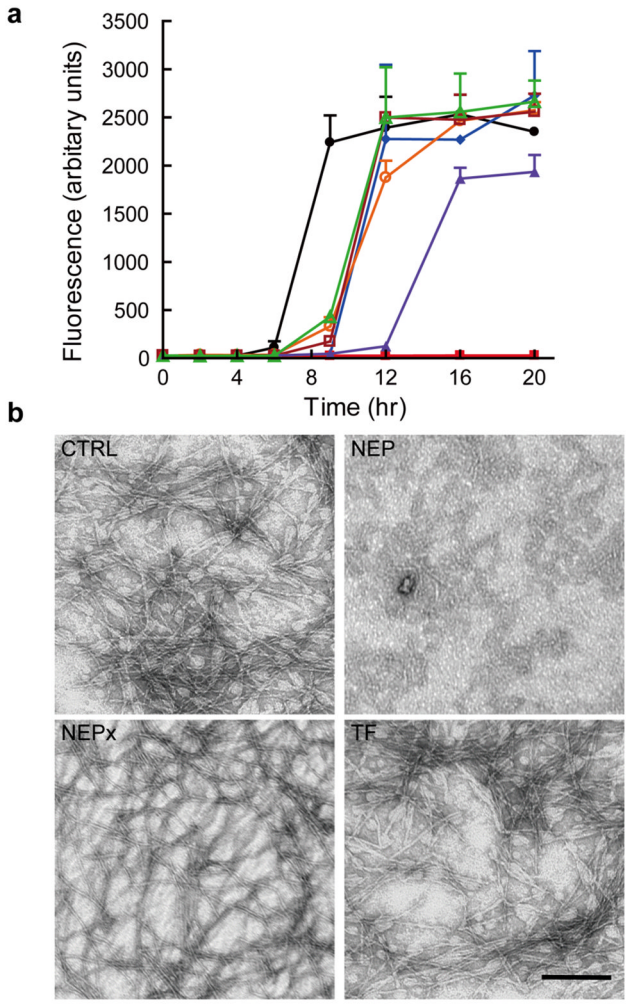

Fig. 2. The effects of NEP and NEPx on hIAPP fibrillization

a. hIAPP (25 μmol/l) was incubated with buffer (filled circle), BSA (filled diamond), transferrin (TF, open circle), NEP (filled square), phosphoramidon treated NEP (open square), NEPx (filled triangle), and phosphoramidon treated NEPx (open triangle) for 20 h at 37°C. Proteins were at 0.5 μmol/l. hIAPP fibrillization was monitored by the change in fluorescence due to thioflavin T binding to fibrils at the indicated time points (n = 3 to 6).

b. Representative TEM images of hIAPP after incubation with buffer (CTRL), NEP, NEPx, or transferrin (TF) at 37°C for 20 h. Scale bar, 200 nm.

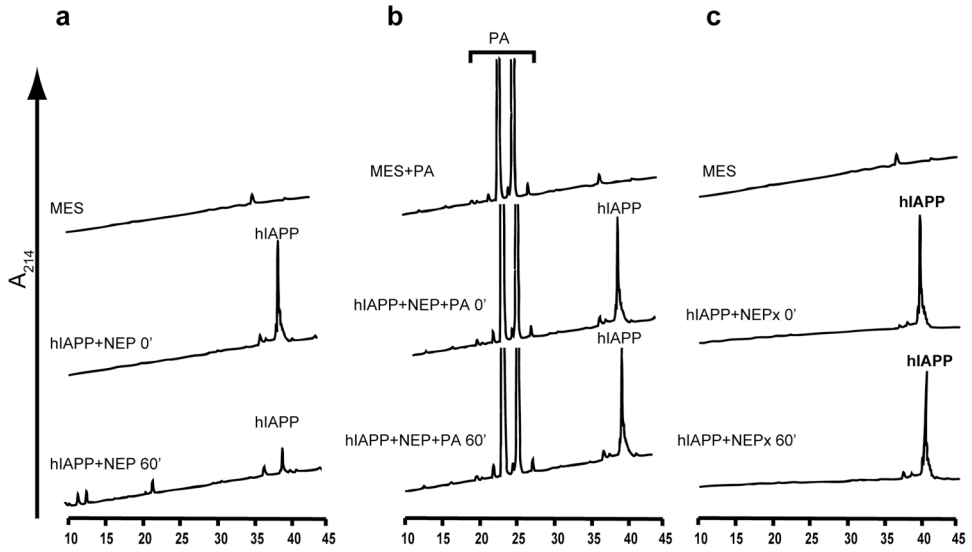

Fig. 3. NEP cleavage of hIAPP

hIAPP (20 μmol/l) was incubated with 400 nmol/l of purified NEP at 37°C for 60 min in the absence (**a**) or presence (**b**) of the NEP inhibitor-phosphoramidon (PA) or 400 nmol/l of catalytically compromised NEP (NEPx) (**c**). Reactions were stopped with 0.5% TFA and analyzed by HPLC as described in Materials and Methods. hIAPP was cleaved by NEP (**a**) but not by PA-treated NEP (**b**) or NEPx (**c**). The large peaks at retention time at 20–30 min in panel b are the phosphoramidon peaks.

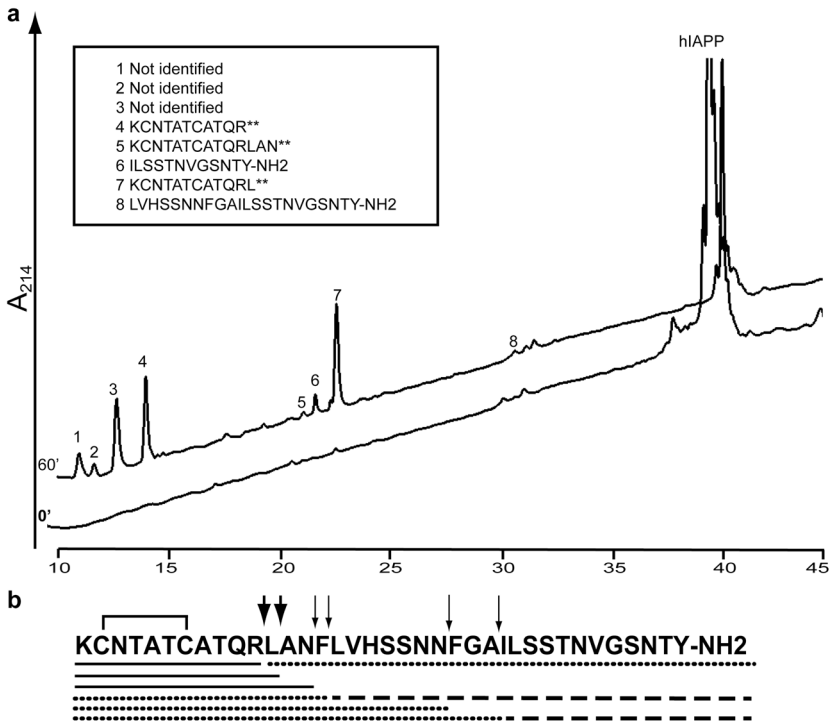

Fig. 4. Identification of NEP cleavage sites in hIAPP

hIAPP (20 μmol/l) was incubated with 400 nmol/l recombinant NEP at 37°C for 60 min. TFA was then added to 0.5% to stop the reaction, which was then subjected to HPLC. Products were collected manually and subjected to mass spectral analysis for identification.

a. HPLC chromatograms of hIAPP incubated with NEP (t = 0) and after incubation at 37°C for 60 min (t = 60). The insert shows the identified degradation products as determined by mass spectrometry.

b. Schematic representation of the cleavage sites on hIAPP. Thick arrows indicate the major cleavage sites while thin arrows indicate minor cleavage sites. Reaction products were confirmed and further extended by direct infusion of a reaction mixture into the mass spectrometer.

The solid line under the hIAPP sequence represents digestion products identified by both HPLC and direct infusion of the reaction mixture while the dashed line represents digestion products identified only by HPLC and the dotted line represents digestion products identified only by direct infusion.

** These products contained oxidized cysteines at positions 2 and 7.

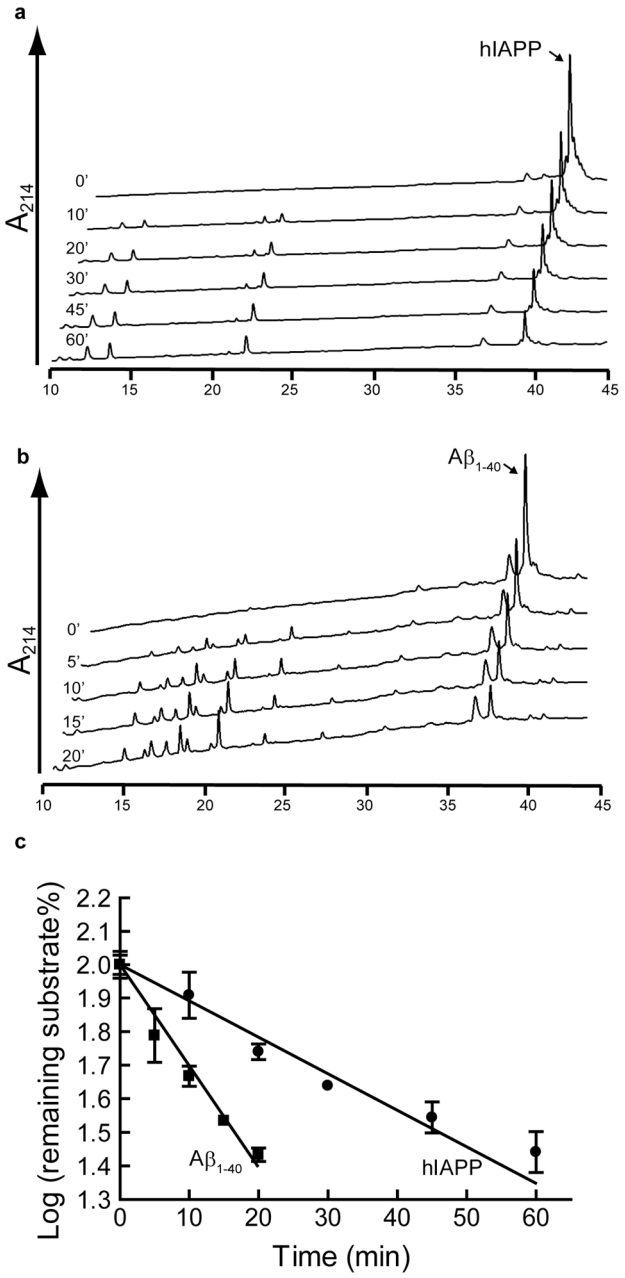

Fig. 5. Comparison of the rates of hIAPP and $A\beta_{1–40}$ degradation by NEP

hIAPP (20 μmol/l) or $A\beta_{1–40}$ (20 μmol/l) was mixed with 400 nmol/l or 40 nmol/l NEP respectively and incubated at 37°C. **a.** HPLC chromatograms of hIAPP degradation by NEP as a function of time. **b.** degradation by NEP as a HPLC chromatograms of $A\beta_{1–40}$ function of time. **c.** Substrate degradation analyzed as a first order plot, hIAPP (circles) ± 0.041 nmols/min/μg NEP or $A\beta_{1–40}$ (squares). The rate of $A\beta_{1–40}$ cleavage is 0.305 while that for hIAPP is 0.010 ± 0.002 nmols/min/μg NEP (n =3).

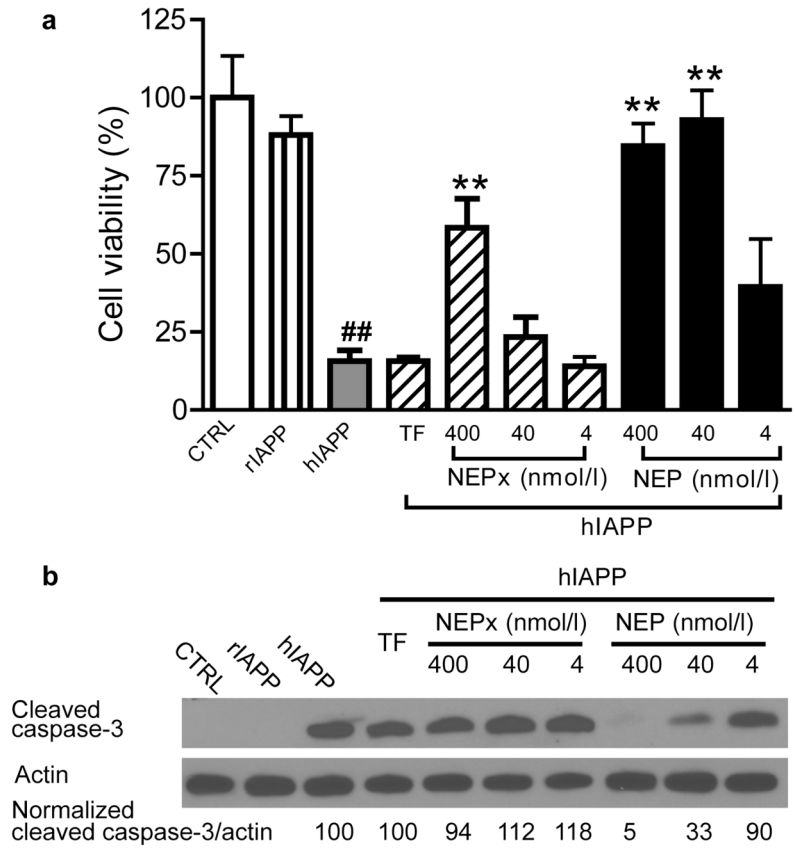

Fig. 6. Effect of recombinant NEP or NEPx on synthetic hIAPP-induced cytotoxicity

Insulinoma INS 832/13 cells were treated with vehicle (0.8% DMSO in media), 20μmol/l synthetic rIAPP or 20 μmol/l synthetic hIAPP along with 4, 40 nmol/l or 400 nmol/l recombinant NEP or NEPx. 400 nmol/l transferrin (TF) was used as control.

a. After treatment for 48 h cell viability was determined using the MTT assay.

$p<0.01$ compared to the vehicle control.

** $P<0.01$ compared to hIAPP alone.

($n = 3$ to 9).

b. Cell apoptosis was evaluated 24 h after treatment with IAPP by following the cleavage and activation of caspase-3 by Western blot analysis. Exogenously added NEP, but not NEPx, reduced cleaved caspase-3 levels induced by synthetic hIAPP.

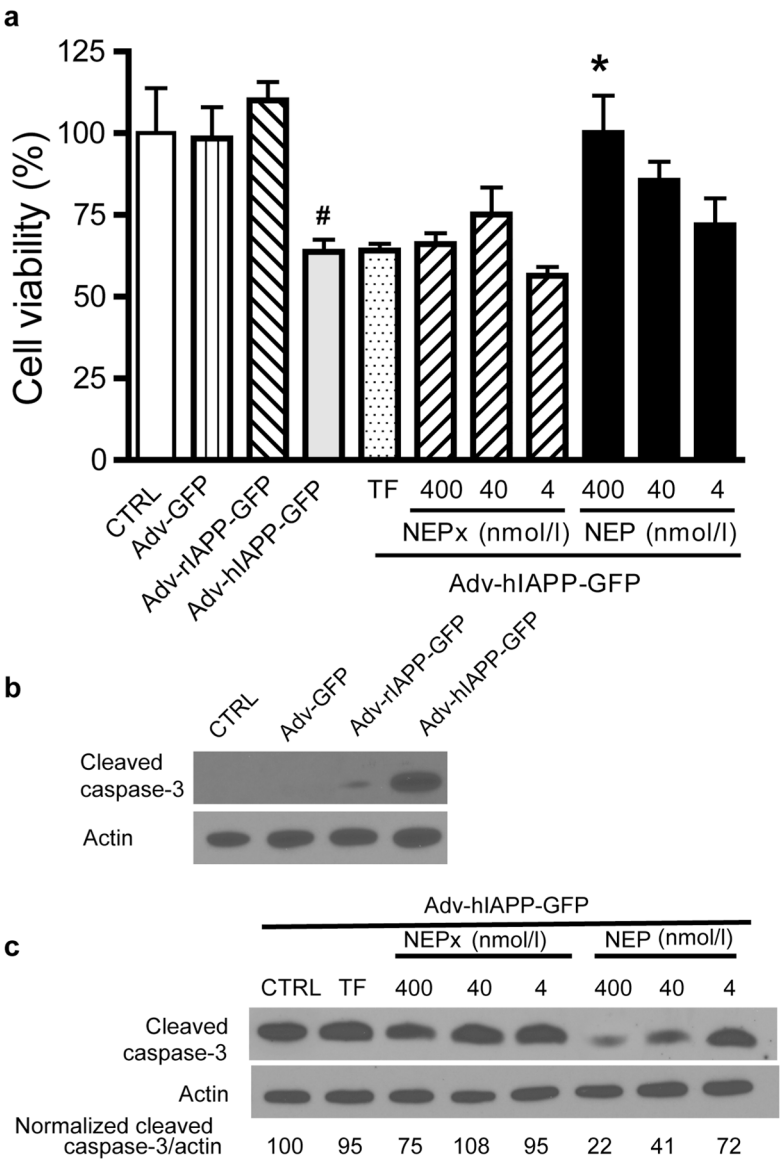

Fig. 7. Effect of recombinant NEP or NEPx on hIAPP overexpression-induced cytotoxicity

Insulinoma INS 832/13 cells were transduced with adenovirus expressing GFP, prepro-rIAPP or prepro-hIAPP fused with a GFP tag at an MOI = 100. To the medias was added 4, 40 nmol/l or 400 nmol/l recombinant NEP or NEPx or 400 nmol/l of transferrin (TF).

a. After 48 h cell viability was determined using the MTT assay.

b. Cell apoptosis was evaluated by following the cleavage and activation of caspase-3 by Western blot analysis 48 h after adenovirus transduction. hIAPP, but not rIAPP or GFP, overexpression induced cleavage and activation of caspase-3 in INS 832/13 cells.

c. Exogenously added NEP reduces cleaved caspase-3 levels induced by hIAPP overexpression. In contrast, only 400 nmol/l NEPx but not 40 and 4 nmol/l NEPx reduces cleaved caspase-3 levels induced by hIAPP overexpression.